Multifluid numerical approximations based on a multipressure formulation.

Christophe Berthon [a,b] Boniface Nkonga [a,b]

[a] *MAB UMR 5466 CNRS, Université Bordeaux I, 351 cours de la libération, 33400 Talence, France.*

[b] *INRIA Futurs, projet ScAlApplix, Domaine de Voluceau-Rocquencourt, B.P. 105, 78153 Le Chesnay Cedex France.*

Abstract

In the present work, we consider the numerical approximations of multifluid compressible flows. We suppose that the flow is composed by non mixing compressible fluids. We propose a dissipative model insuring, for the mixture, the conservation of the mass, the momentum and the total energy. Entropy balances between phases are described by additional nonconservative equations. At the limit of vanishing viscosity the model is still consistent with the entropy balances. The nonlinear projection scheme is used to preserve, at the discrete level, the main properties of the model. Numerical experiments are conducted to validate the proposed models for the multicomponent shock tube, the bubble-shock interaction and the tank filling problems.

Key words: compressible multifluid flows, nonconservative equations, finite volume methods, nonlinear projection methods.

1 Introduction

Modeling and computing multifluid flows is a very active research area. This is due to the fact that multifluid flows play fundamental roles in many natural phenomena used in industrial processes. Compressible multifluid flows occur when the flow is composed by fluids of different physical properties, separated by interfaces. One of the classical examples is the behavior of the interface between two different gases under a shock [22].

For the multiphase and multifluid flows models developed by Saurel and Abgrall [6], the size of the model grows with the number of flow components. This model is well posed in general, but turns out to be efficient only for flows

with fews components. On the other hand, simplified models [2,4,36] needs to be approximated properly in order to avoid spurious waves. In any case, numerical result obtained with simplified models do not always recover the physical temperature profile [29]. The compromise proposed in [29] was to use as variables of the modelization the volumes fractions, the partial densities, the momentum and the total energy of the mixture: $(\alpha_k,\ \rho_k,\ \rho\mathbf{u},\ E)$. The numerical approximations was then achieved by some technics proposed in [3,6,24]. However, it is implicitly assumed in these modelizations that pressure and velocity relaxations are instantaneous. The aim of this paper is to propose a numerical modelization of non mixing compressible multimaterials flows that will still available when isobaric approximation fails.

Following strategies used in ionized plasma [17] and as an extension of the multifluid model developed in [25], we consider a diffusive model using as variables the total density, the total momentum, the partial energies and the mass fractions: $(\rho,\ \rho\mathbf{u},\ \rho_k e_k,\ Y_k)$. This modelization use some basic properties of the non mixing flows proposed in [26]. However, as many other models in multifluid flows [4,7,29], the derived system is partially non conservative. The non conservative form of the system is known to be crucial (Dal Maso, LeFloch and Murat [18] or Hou and LeFloch [23]) since the system is not defined in the sense of distributions as soon as the solutions are discontinuous. This unacceptable problem find large numerical repercussions as emphasized in [23]. Raviart and Sainsaulieu [34] have proposed a diffusive approach for modeling spray. From the diffusive operator, they propose, after the work of Dal Maso, LeFloch and Murat [18], a weak definition of discontinuous solutions but for a conditionally hyperbolic system. As Raviart and Sainsaulieu [34], our model is diffusive and thus ensures a relevant definition of discontinuous solutions [9,18]. Since each phase is assumed to be hyperbolic, the system of PDEs is, in addition, unconditionally hyperbolic. Moreover, an Eulerian extension is proposed. The (k,ϵ) turbulence model (see Mohammadi and Pironneau [30], Larrouturou and Olivier [28]) is very closed to our model form. Therefore, extensions of our model for turbulent multifluid flow are straightforward. Indeed, some phenomena in multifluid flows, as particles rotations or bubble pulsation, can be modeled by turbulence like models [8].

In the following sections, the physical model is formulated in the multi-pressure form with viscous effects. We then deduce a conservative formulation of the total energy supplemented by non conservative entropy balance equations. Modeling closures in multiphase and multifluid are proposed. The vanishing viscosity limit of the model is established. Relationship with the (k,ϵ) turbulent model is achieved. The numerical nonlinear projection method is applied to the 1D problems and extended, in the finite volumes approximations on unstructured meshes, to multidimensional problems with external forces source terms. Both 1D and 2D applications are performed for a multifluid shock tube (1D), bubble-shock interactions (2D) and tank filling (2D).

2 The physical model

We consider a multifluid flow governed by the compressible Navier-Stokes equations. For simplicity, the physical model, in this section, is developed in one space dimension for a mixture defined by $n_p \geq 2$ fluid components. Extension to multi-dimensional problem is proposed in Section 4.

In order to derive the physical model, we denote by $\rho > 0$ the total density and by ρu the total momentum of the mixture. We assume that, locally, the components of the mixture are separated: non mixing fluids. However, in a caracteristic volume of the modelisation, many components can be present. We denote by ρ_k, $Y_k = \frac{\rho_k}{\rho}$ and v_k respectively the partial density, the mass fraction and the specific volume fraction. The closure for v_k is given below, but generally we have $v_k \neq \frac{1}{\rho_k}$ exepted for very specific model. We assume that all the gases components of the mixture have the same velocity u. The pressure p_k of a given component is a function of v_k and e_k the internal energy of the component. According to our target applications, we assume that the thermal conductivity coefficient is negligible. Therefore, we propose the following model:

$$\begin{cases} \partial_t \rho + \partial_x \rho u = 0, \\ \partial_t(\rho u) + \partial_x(\rho u^2 + p) = \partial_x(\mu \partial_x u), \\ \partial_t(\rho_k e_k) + \partial_x(\rho_k e_k u) + \tilde{p}_k \partial_x u = \tilde{\mu}_k (\partial_x u)^2, \quad \text{for} \quad k = 1,\ n_p, \end{cases} \tag{1}$$

where $e_k = e_k(v_k, p_k)$ is defined by the physics. The partial pressure $\tilde{p}_k \neq p_k$ and the viscosity coeficients $\tilde{\mu}_k$ will be defined latter. In any case, the model will recover the usual equation for the total energy conservation:

$$\partial_t E + \partial_x (E + p)u = \partial_x(\mu u \partial_x u) \quad \text{where} \quad E = \sum_k \rho_k e_k + \frac{1}{2}\rho u^2 \tag{2}$$

$$\text{with} \quad p = \sum_k \tilde{p}_k \quad \text{and} \quad \mu = \sum_k \tilde{\mu}_k. \tag{3}$$

According to analysis performed in [26] for non mixing fluids, we have:

$$D_t Y_k = 0 \quad \text{and} \quad \sum_k Y_k v_k = \frac{1}{\rho} = v \tag{4}$$

where v denotes the total specific volume and $D_t\phi = \partial_t \phi + u \partial_x \phi$ is the material derivative of the quantity ϕ. In addition let us emphasis that $0 \leq Y_k \leq 1$ and

$\sum_k Y_k = 1$. The system (1) then take the following form:

$$\begin{cases} D_t\rho = -\rho\partial_x u, \\ \rho D_t u + \partial_x p = \partial_x(\mu\partial_x u), \\ \rho D_t \tilde{e}_k + \tilde{p}_k\partial_x u = \tilde{\mu}_k(\partial_x u)^2, \quad \text{for} \quad k = 1,\ n_p, \end{cases}$$

where $\tilde{e}_k = Y_k e_k$.

Let us denote by s_k the specific entropy of a given component. The second law of the thermodynamic, for each component of the fluid, is written as:

$$de_k = -T_k ds_k - p_k dv_k, \tag{5}$$

where $T_k > 0$ is the temperature. In the present work s_k is the mathematical entropy instead of $-s_k$ which denotes the physical entropy (see Godlewski and Raviart [20] to further details). As usual, the functions $(v_k, s_k) \to e_k(v_k, s_k)$ are assumed to be strictly convex and satisfy:

$$\frac{\partial e_k}{\partial v_k}(v_k, s_k) = -p_k < 0 \quad \text{and} \quad \frac{\partial e_k}{\partial s_k}(v_k, s_k) = -T_k < 0. \tag{6}$$

Therefore, according the modelling assumsions proposed in [26], we have the following result:

Lemma 1 *Assume that there exist a set of parameters $\lambda_k > 0$ such that*

$$D_t v_k = \lambda_k D_t v. \tag{7}$$

Smooth solutions of (1)–(7) satisfy a conservation law for the total energy (energy balance):

$$\partial_t E + \partial_x(E + p)u = \partial_x(\mu u\partial_x u) \quad \textit{where} \quad p = \sum_k \tilde{p}_k \tag{8}$$

In addition, let us assume $\tilde{p}_k = p_k Y_k \lambda_k$ and $\tilde{\mu}_k = Y_k\mu_k$, where $\mu_k \geq 0$ is a parameter function to be defined. Then, we have the following entropy inequalities:

$$\partial_t \rho s_k + \partial_x \rho s_k u = -\frac{\mu_k}{T_k}(\partial_x u)^2 \leq 0, \quad k = 1,\ n_p. \tag{9}$$

As a consequence, we obtain the following entropy balance equation holds for $k = 1,\ n_p - 1$:

$$\frac{\mu_{n_p}}{T_{n_p}}\left\{\partial_t \rho s_k + \partial_x \rho s_k u\right\} - \frac{\mu_k}{T_k}\left\{\partial_t \rho s_{n_p} + \partial_x \rho s_{n_p} u\right\} = 0, \tag{10}$$

For perfect gas, if we assume in addition that $\lambda_k = \frac{v_k}{v}$*, then we have:*

$$\partial_t \rho \tilde{s}_k + \partial_x \rho \tilde{s}_k u = -\frac{\mu_k}{T_k}(\partial_x u)^2 \leq 0, \quad k = 1,\ n_p, \tag{11}$$

where $\tilde{s}_k(\rho, \tilde{p}_k) = -\log\left(\frac{\tilde{p}_k}{\rho^{\gamma_k}}\right)$ *and* $T_k = p_k v_k/(\gamma_k - 1)$*. As a consequence, we have for all* $1 \leq k \leq n_p - 1$*:*

$$\frac{\beta_{n_p}}{T_{n_p}}\left\{\partial_t \rho \tilde{s}_k + \partial_x \rho \tilde{s}_k u\right\} - \frac{\beta_k}{T_k}\left\{\partial_t \rho \tilde{s}_{n_p} + \partial_x \rho \tilde{s}_{n_p} u\right\} = 0, \tag{12}$$

where we have introduced $\beta_k = \dfrac{\mu_k}{\sum_\ell \mu_\ell}$*.*

Before we establish the above result, let us note that several choice for the closure of λ_k is possible. For instance, after the following proof, the reader will easily convince that $\lambda_k = 1/Y_k$ can be considered. This specific closure will be usefull in the framework of turbulent model.

Proof. First, we establish the identity (9). Since we have:

$$\rho Y_k D_t e_k + \tilde{p}_k \partial_x u = \tilde{\mu}_k (\partial_x u)^2,$$

we deduce from (6):

$$-\rho Y_k p_k D_t v_k - \rho Y_k T_k D_t s_k + \tilde{p}_k \partial_x u = \tilde{\mu}_k (\partial_x u)^2.$$

Now, we have $D_t v_k = \lambda_k D_t(1/\rho) = \frac{\lambda_k}{\rho}\partial_x u$ to obtain:

$$-\rho Y_k T_k D_t s_k + (\tilde{p}_k - Y_k \lambda_k p_k)\partial_x u = \tilde{\mu}_k (\partial_x u)^2.$$

Owing to the definition of $\tilde{p}_k$ and $\tilde{\mu}_k$, (9) is proved.

Next, we focus on (11). First, we note that $D_t \lambda_k = 0$ as soon as $\lambda_k = v_k/v$. Indeed, we have

$$D_t \lambda_k = \frac{1}{v} D_t v_k - \frac{v_k}{v^2} D_t v = \frac{1}{v^2}(\lambda_k v - v_k) D_t v = 0.$$

Now, for perfect gas we have $e_k(v_k, s_k) = \mathrm{e}^{-s_k}/((\gamma_k - 1)v_k^{\gamma_k - 1})$ and then $s_k = -\log p_k v_k^{\gamma_k}$ and $T_k = p_k v_k/(\gamma_k - 1)$. The equation (11) is a direct consequence

of

$$D_t s_k = -D_t \log \frac{\tilde{p}_k}{\rho^{\gamma_k}} + D_t \log \frac{(v_k \rho)^{\gamma_k}}{\lambda_k Y_k},$$

where $D_t \lambda_k = 0$, $D_t Y_k = 0$ and $v_k \rho = \lambda_k$. The proof is thus completed. $\square$

For the sake of simplicity in the sequel, the system (1)–(7) will be considered always in the case of perfect gaz.

Except for restrictive assumptions (see [10]), the system (1) never reads under conservation form. As a consequence of the non conservation form, the system (1) does not admit a weak formulation and thus we cannot characterize shock wave solutions by the usual Rankine-Hugoniot conditions. In Dal Maso, LeFloch and Murat [18] or Raviart and Sainsaulieu [34], the authors propose a weak definition based on the existence of traveling wave solutions. Moreover, under thermodynamic properties (systematically satisfied for perfect gas), the existence and the uniqueness of traveling waves are proved in [9,11].

Since the total pressure $p = \sum_k \rho^{\gamma_k} \mathrm{e}^{-\tilde{s}_k}$ satisfies $\frac{\partial p}{\partial \rho} > 0$, we have the following stability result:

Lemma 2 *The first order extracted system from (1) is hyperbolic. The eigenvalues are $u - c$, $u + c$ and u where $c^2 = \frac{\partial p}{\partial \rho}$. The field associated with the eigenvalues $u \pm c$ are genuinely nonlinear while the field associated with the eigenvalue u is linearly degenerate. In addition, across a contact wave, the velocity u and the total pressure p are continuous.*

To summarize, the energy and the entropy balance equations (see Lemma 1) are used to reformulate the non conservative system (1) under the following equivalent form:

$$\begin{cases} \partial_t \rho + \partial_x \rho u = 0, \\ \partial_t \rho u + \partial_x (\rho u^2 + p) = \partial_x (\mu \partial_x u), \\ \partial_t E + \partial_x (E + p) u = \partial_x (\mu u \partial_x u), \\ \frac{\beta_{n_p}}{T_{n_p}} \left\{ \partial_t \rho \tilde{s}_k + \partial_x \rho \tilde{s}_k u \right\} - \frac{\beta_k}{T_k} \left\{ \partial_t \rho \tilde{s}_{n_p} + \partial_x \rho \tilde{s}_{n_p} u \right\} = 0, \quad k = 1,\ n_p - 1. \end{cases} \tag{13}$$

In the sequel, this equivalent system will be suitable for analytical and numerical analysis.

According to the entropy balance equation, the entropy $\tilde{s}_{n_p}$ is a function of the unknowns $(\rho, \rho u, E, \rho \tilde{s}_1, ..., \rho \tilde{s}_{n_p - 1})$. Therefore, the reformulation of the

entropy $\tilde{s}_{n_p}$ is:

$$\tilde{s}_{n_p} = -\log\left(\frac{\gamma_{n_p}-1}{\rho^{\gamma_{n_p}}}\left(E-\rho\frac{u^2}{2}-\sum_{k=1}^{n_p-1}\frac{\rho^{\gamma_k}}{\gamma_k-1}\mathrm{e}^{-\tilde{s}_k}\right)\right).$$

In [9] it is proved that, for a fixed $\bar{k}$, if $\mu_{\bar{k}}$ goes to zero (the associated $\beta_{\bar{k}}$ goes to zero), then the traveling wave solutions of (13) are also solutions of the following system:

$$\begin{cases} \partial_t\rho + \partial_x\rho u = 0, \\ \partial_t\rho u + \partial_x(\rho u^2 + p) = \partial_x(\mu\partial_x u), \\ \partial_t E + \partial_x(E+p)u = \partial_x(\mu u\partial_x u), \\ \partial_t\rho\tilde{s}_{\bar{k}} + \partial_x\rho\tilde{s}_{\bar{k}}u = 0, \\ \frac{\beta_{n_p}}{T_{n_p}}\left\{\partial_t\rho\tilde{s}_k + \partial_x\rho\tilde{s}_k u\right\} - \frac{\beta_k}{T_k}\left\{\partial_t\rho\tilde{s}_{n_p} + \partial_x\rho\tilde{s}_{n_p}u\right\} = 0,\ 1\le k\neq\bar{k}\le n_p-1. \end{cases} \tag{14}$$

In additiopn, if for $k = 1,\ n_p - 1$ the volume fractions Y_k go to zero, the continuity assumption say that the volume fraction Y_{n_p} of the last component goes to one and the system (13) reduce to the Navier-Stokes equations for the component n_p, completed by an independent transport equation for the entropy of the other components.

3 Modeling closures

In our model (13), we have to define the evolution of the parameters β_k (or equivalently μ_k). In the present section, we propose several models for the computation of β_k. Some of them lead to usual physical models (see Drew and Passman [19] or Massoni et al. [29]).

3.1 A bifluid model

Let us assume here that the viscosities are a product of the characteristic viscosity of the phase by a function of the partial temperature. In the present work, we consider the following arbitrary choice:

$$\mu_1 = (Y_1T_1)^{m_1}\bar{\mu}_1 \qquad \text{and} \qquad \mu_2 = (Y_2T_2)^{m_2}\bar{\mu}_2,$$

where $m_1 > 0$ and $m_2 > 0$ are real constants to be fixed. Then, when the partial temperatures are given ($\tilde{T}_k = Y_kT_k = \tilde{p}_k v/(\gamma_k - 1)$), the variables β_k

can be computed as follows:

$$\beta_k(\tilde{T}_1,\tilde{T}_2)=\frac{(\tilde{T}_k)^{m_k}\bar{\mu}_k}{(\tilde{T}_1)^{m_1}\bar{\mu}_1+(\tilde{T}_2)^{m_2}\bar{\mu}_2}. \tag{15}$$

Each β_k is a *temperature fraction* characterizing material interfaces. To fix the idea, let us consider the particular case where $\bar{\mu}_1$ and $\bar{\mu}_2$ are constant. The final model thus reads:

$$\begin{cases}
\partial_t\rho+\partial_x\rho u=0,\\
\partial_t\rho u+\partial_x(\rho u^2+p)=\partial_x(\mu\partial_x u),\\
\partial_t E+\partial_x(E+p)u=\partial_x(\mu u\partial_x u),\\
\partial_t\rho Y_1+\partial_x\rho Y_1 u=0,\\
\frac{\beta}{T_2}\left\{\partial_t\rho\tilde{s}_1+\partial_x\rho\tilde{s}_1 u\right\}-\frac{(1-\beta)}{T_1}\left\{\partial_t\rho\tilde{s}_2+\partial_x\rho\tilde{s}_2 u\right\}=0,\\
\beta(\tilde{T}_1,\tilde{T}_2)=\frac{(\tilde{T}_2)^{m_2}}{\bar{\mu}(\tilde{T}_1)^{m_1}+(\tilde{T}_2)^{m_2}},
\end{cases} \tag{16}$$

where we have set $\bar{\mu}=\bar{\mu}_1/\bar{\mu}_2$. Let us note that the model under consideration turns out to be uncoupled of the evolution of v_k and λ_k. Indeed, in the above system, we need evaluate β_k/T_k but as soon as $Y_k\neq 0$ we have $\tilde{T}_k=Y_kT_k=\tilde{p}_kv/(\gamma_k-1)$. Now, if $Y_k=0$ then $\beta_k=0$ and, since by definition $T_k>0$, we obtain $\beta_k/T_k=0$.

We propose to derive the above models in the framework of large Reynolds numbers. In the above models, note that the fraction β_k is independent of the Reynolds number but depend on the ratios of viscosities. We thus propose:

$$\begin{cases}
\partial_t\rho+\partial_x\rho u=0,\\
\partial_t\rho u+\partial_x(\rho u^2+p)=0,\\
\partial_t\rho E+\partial_x(\rho E+p)u=0,\\
\partial_t\rho Y_1+\partial_x\rho Y_1 u=0,\\
\frac{\beta_{n_p}}{T_{n_p}}\left\{\partial_t\rho\tilde{s}_k+\partial_x\rho\tilde{s}_k u\right\}-\frac{\beta_k}{T_k}\left\{\partial_t\rho\tilde{s}_{n_p}+\partial_x\rho\tilde{s}_{n_p}u\right\}=0,
\end{cases} \tag{17}$$

with

$$0\leq\beta_k=\lim_{\mu_j\to 0,\ j=1,n_p}\frac{\mu_k}{\sum_\ell\mu_\ell}\leq 1.$$

We have assumed that all the viscosities decrease to zero with the same speed. At this limit, the model recover the usual Euler equations with additional entropy balance equations. The mean pressure is then obtained from these equations. This is an implicit closure of the mean pressure based on entropy

balance. Contrary to the models proposed in [29], this model do not assume a pressure or a temperature equilibrium.

3.2 Turbulent models

A turbulent flow described by the (k, ϵ) model (for instance see Mohammadi and Pironneau[30]), is governed by the following equations:

$$\begin{cases} \partial_t \rho + \partial_x \rho u = 0, \\ \partial_t \rho u + \partial_x (\rho u^2 + p + \frac{2}{3}\rho k) = \partial_x((\mu + \mu_t)\partial_x u), \\ \partial_t E + \partial_x (E + p + \frac{2}{3}\rho k)u = \partial_x((\mu + \mu_t)u\partial_x u), \\ \partial_t \rho k + \partial_x \rho k u + \frac{2}{3}\rho k \partial_x u = \mu_t (\partial_x u)^2 - \rho\epsilon, \\ \partial_t \rho\epsilon + \partial_x \rho\epsilon u + C_1 \frac{2}{3}\rho\epsilon\partial_x u = C_1 \mu_t \frac{\epsilon}{k}(\partial_x u)^2 - C_2 \rho \frac{\epsilon^2}{k}, \end{cases} \tag{18}$$

where k is the kinetic turbulent energy and ϵ the dissipation rate of k. The total energy E and the turbulent viscosity μ_t are defined by

$$E = \rho\frac{u^2}{2} + \rho e + \rho k, \quad \mu_t = C_\mu \rho \frac{k^2}{\epsilon},$$

with C_μ, C_1 and C_2 modeling constants. The pressure p and the specific internal energy e of the gas are defined by the Gibbs law:

$$de = -T\ ds - p\ dv,$$

where $T > 0$ denotes the temperature and $v = 1/\rho$ is the specific volume. When the source terms are neglected, following the calculations proposed in [9], we rewrite equivalently the system as follows:

$$\begin{cases} \partial_t \rho + \partial_x \rho u = 0, \\ \partial_t \rho u + \partial_x (\rho u^2 + p + \frac{2}{3}\rho k) = \partial_x((\mu + \mu_t)\partial_x u), \\ \partial_t \rho E + \partial_x (\rho E + p + \frac{2}{3}\rho k)u = \partial_x((\mu + \mu_t)u\partial_x u), \\ \frac{\beta}{T_t}\{\partial_t \rho s + \partial_x \rho s u\} - \frac{1-\beta}{T}\{\partial_t \rho s_t + \partial_x \rho s_t u\} = 0, \\ \partial_t \rho \frac{k^{c_1}}{\epsilon} + \partial_x \rho \frac{k^{c_1}}{\epsilon} u = 0, \end{cases} \tag{19}$$

where

$$s_t = -\log\frac{p_t}{\rho^{\gamma_t}}, \quad T_t = \frac{p_t}{\rho(\gamma_t - 1)}, \quad p_t = \frac{2}{3}\rho k, \quad \beta = \frac{\mu_t}{\mu + \mu_t}, \quad \gamma_t = \frac{5}{3}.$$

Defining the turbulent pressure by $p_t = \frac{2}{3}\rho k$, we recover the model (13) completed by a transport equation for $\frac{k^{c_1}}{\epsilon}$ as soon as $\lambda_k = 1/Y_k$. Indeed, a flow is composed by laminar and turbulent components. The laminar component is characterized by its specific internal energy e and pressure p. The turbulent component is characterized by its specific internal energy $e_t = k$ and pressure $p_t = (\gamma_t - 1)\rho e_t$.

4 Numerical approximation

This section is devoted to a nonstandard finite volume method to approximate the solutions of the nonconservative system (13). The principle of this method, called "nonlinear projection method", is described in [10] (see also [15]). This method is presented in this section in the context of the bifluid model. Let us reformulate the system (16) as:

$$\partial_t \mathbf{w} + \partial_x \mathbf{f}(\mathbf{w}, \rho\tilde{s}_1, \rho\tilde{s}_2) = 0 \tag{20}$$

$$\frac{\beta}{T_2}\left\{\partial_t \rho\tilde{s}_1 + \partial_x \rho\tilde{s}_1 u\right\} - \frac{(1-\beta)}{T_1}\left\{\partial_t \rho\tilde{s}_2 + \partial_x \rho\tilde{s}_2 u\right\} = 0, \tag{21}$$

$$\beta = \beta(\tilde{T}_1, \tilde{T}_2) = \frac{(\tilde{T}_2)^{m_2}}{(\tilde{T}_2)^{m_2} + \bar{\mu}(\tilde{T}_1)^{m_1}}, \tag{22}$$

where $\mathbf{w} = {}^t(\rho, \rho u, E, \rho Y_1)$ and $\mathbf{f}(\mathbf{w}) = {}^t(\rho u, \rho u^2 + p, (E+p)u, \rho Y_1 u)$.

The principle of the nonlinear projection method is to approximate this system by a two steps splitting technique:

First step: Time evolution. For given $\mathbf{w}^n$, $\tilde{s}_1^n$ and $\tilde{s}_1^n$, the following conservative system is approximated:

$$\begin{cases} \partial_t \mathbf{w} + \partial_x \mathbf{f}(\mathbf{w}, \rho\tilde{s}_1, \rho\tilde{s}_2) = 0 \\ \quad \partial_t \rho\tilde{s}_1 + \partial_x \rho\tilde{s}_1 u = 0 \qquad \Longrightarrow \mathbf{w}^{n+1}, \quad \tilde{s}_1^{n+\frac{1}{2}}, \quad \tilde{s}_2^{n+\frac{1}{2}}. \\ \quad \tilde{s}_2 = \tilde{s}_2(\mathbf{w}, \rho\tilde{s}_1) \end{cases} \tag{23}$$

This is a prediction step for the partial entropies. The function $\rho\tilde{s}_2$ is an entropy of this system and satisfy the inequality:

$$\partial_t \rho\tilde{s}_2 + \partial_x \rho\tilde{s}_2 u \leq 0.$$

Second step: Nonlinear projection. The variables $\mathbf{w}^{n+1}$ computed in the

previous step are preserved and the entropy balance is enforced:

$$\left\{\begin{array}{c} \partial_t \mathbf{w} = 0, \quad \tilde{s}_2 = \tilde{s}_2(\mathbf{w}, \rho\tilde{s}_1) \\ \frac{\beta}{T_2}\left\{\partial_t \rho\tilde{s}_1 + \partial_x \rho\tilde{s}_1 u\right\} - \frac{(1-\beta)}{T_1}\left\{\partial_t \rho\tilde{s}_2 + \partial_x \rho\tilde{s}_2 u\right\} = 0, \\ \beta = \beta(\tilde{T}_1, \tilde{T}_2), \end{array}\right.$$

$$\Longrightarrow \mathbf{w}^{n+1}, \quad \tilde{s}_1^{n+1}, \quad \tilde{s}_2^{n+1}.$$

We now propose a numerical approximation of the different steps of the method.

4.1 The 1-D case

We consider a structured mesh in space and time, defined by the cells $I_i =]x_{i-\frac{1}{2}}, \quad x_{i+\frac{1}{2}}[$ and the time intervals $[t^n, \quad t^{n+1}[$:

$$t^n = n\Delta t \quad \text{and} \quad x_{i+\frac{1}{2}} = (i + \frac{1}{2})\Delta x,$$

where Δt is the time step and Δx the cells length. Approximate solution, at time t^n, will be constant in each cells I_i. For the variable $\mathbf{w}$, for example, we denote by $\mathbf{w}_i^n$ the approximate value at time t^n in cell I_i. The numerical solution $\mathbf{w}_h^n(x) = \mathbf{w}_h(x, t^n)$ is then defined by:

$$\mathbf{w}_h^n(x) = \mathbf{w}_i^n \quad \text{when} \quad x \in I_i.$$

Under the CFL like condition:

$$\frac{\Delta t}{\Delta x} \max |\lambda_i(\mathbf{w})| \leq \frac{1}{2}, \tag{24}$$

the solution of the Cauchy problem of the system (23) with the initial data $\mathbf{w}_h^n(x)$ is composed by the solutions of non interacting elementary Riemann problems at the cells interfaces. Let us denote by $\mathbf{w}_{i+\frac{1}{2}}(\xi)$ and $(\rho\tilde{s}_1)_{i+\frac{1}{2}}(\xi)$ the exact or the approximated solution of the elementary Riemann problem centered at $x_{i+\frac{1}{2}}$:

$$\begin{array}{r} \mathbf{w}_{i+\frac{1}{2}}(\xi) = W\left(\xi, \mathbf{w}_i^n, (\rho\tilde{s}_1)_i^n, \mathbf{w}_{i+1}^n, (\rho\tilde{s}_1)_{i+1}^n\right) \\ (\rho\tilde{s}_1)_{i+\frac{1}{2}}(\xi) = S\left(\xi, \mathbf{w}_i^n, (\rho\tilde{s}_1)_i^n, \mathbf{w}_{i+1}^n, (\rho\tilde{s}_1)_{i+1}^n\right) \end{array} \quad \text{with} \quad \xi = \frac{x - x_{i+\frac{1}{2}}}{t - t^n}.$$

The Godunov method is obtained by the projection of the solution composed of elementary Riemann problems on the space of piecewise constants functions

on the cells. This is achieved by an averaging over each cell [20]. Let us define the numerical flux by:

$$\begin{aligned}
\phi^{\mathbf{w}}_{i+\frac{1}{2}} &= \mathbf{f}\left(\mathbf{w}_{i+\frac{1}{2}}(0), \quad (\rho\tilde{s}_1)_{i+\frac{1}{2}}(0), \quad (\rho\tilde{s}_2)(\mathbf{w}_{i+\frac{1}{2}}(0),\ (\rho\tilde{s}_1)_{i+\frac{1}{2}}(0))\right), \\
\phi^{\rho\tilde{s}_1}_{i+\frac{1}{2}} &= (\tilde{s}_1)_{i+\frac{1}{2}}(0)\phi^{\rho}_{i+\frac{1}{2}},
\end{aligned}$$

where $\phi^{\rho}_{i+\frac{1}{2}}$ is the first component of $\phi^{\mathbf{w}}_{i+\frac{1}{2}}$ and $(\tilde{s}_1)_{i+\frac{1}{2}}(\xi) = \frac{(\rho\tilde{s}_1)_{i+\frac{1}{2}}(\xi)}{\rho_{i+\frac{1}{2}}(\xi)}$. Then the numerical scheme in the conservative step is:

$$\begin{aligned}
\mathbf{w}_i^{n+1} &= \mathbf{w}_i^n \quad -\frac{\Delta t}{\Delta x}\left(\phi^{\mathbf{w}}_{i+\frac{1}{2}} - \phi^{\mathbf{w}}_{i-\frac{1}{2}}\right), \\
(\rho\tilde{s}_1)_i^{n+\frac{1}{2}} &= (\rho\tilde{s}_1)_i^n - \frac{\Delta t}{\Delta x}\left(\phi^{\rho\tilde{s}_1}_{i+\frac{1}{2}} - \phi^{\rho\tilde{s}_1}_{i-\frac{1}{2}}\right).
\end{aligned} \tag{25}$$

The convex entropy of the system (23), $\{\rho\tilde{s}_2\}(\mathbf{w}_i^{n+1}, (\rho\tilde{s}_1)_i^{n+1})$ satisfies a discrete entropy inequality:

$$\{\rho\tilde{s}_2\}(\mathbf{w}_i^{n+1}, (\rho\tilde{s}_1)_i^{n+\frac{1}{2}}) - (\rho\tilde{s}_2)_i^n + \frac{\Delta t}{\Delta x}\left(\phi^{\rho\tilde{s}_2}_{i+\frac{1}{2}} - \phi^{\rho\tilde{s}_2}_{i-\frac{1}{2}}\right) \leq 0, \tag{26}$$

where

$$\phi^{\rho\tilde{s}_2}_{i+\frac{1}{2}} = \tilde{s}_2(\mathbf{w}_{i+\frac{1}{2}}(0),\ (\rho\tilde{s}_1)_{i+\frac{1}{2}}(0)))\phi^{\rho}_{i+\frac{1}{2}}.$$

Moreover, the positiveness of $(\tilde{\epsilon}_1)_i^{n+\frac{1}{2}}$ and $(\tilde{\epsilon}_2)_i^{n+\frac{1}{2}}$ is ensured as soon as the density ρ_i^{n+1} is positive.

In general, the rate of the entropy dissipation associated to $\rho\tilde{s}_2$ is strictly negative. Indeed the L^2 projection cannot be preserved. Indeed, by the Jensen inequality, we have:

$$\{\rho\tilde{s}_2\}(\mathbf{w}_i^{n+1}, \{\rho\tilde{s}_1^{n+\frac{1}{2}}\}) \leq \frac{1}{\Delta x}\int_{x_{i-1/2}}^{x_{i+1/2}} \{\rho\tilde{s}_2\}\left(\mathbf{w}, \rho\tilde{s}_1\right)(x, t^{n+\frac{1}{2}})dx. \tag{27}$$

This means that, the dissipation of the entropy $\{\rho\tilde{s}_2\}$ is strictly negative. On the other hand, the specific entropy $\tilde{s}_1$ is simply advected by the flow and therefore, is preserved by the classical (L^2) projection step. At the discrete level, this discrepancy results cause the failure of the entropy balance equation (12). In the second step, the entropy dissipation is redistribute in order to enforce the balance (12). Therefore, $(\rho\tilde{s}_1)_i^{n+1}$ is computed from a discrete approximation of the entropy balance equation:

$$\frac{\beta_i}{(T_2)_i^{n+1/2}}\Big(\{\rho\tilde{s}_2\}(\mathbf{w}_i^{n+1},(\rho\tilde{s}_1)_i^{n+1})-(\rho\tilde{s}_2)_i^{n+\frac{1}{2}}\Big)- \frac{1-\beta_i}{(T_1)_i^{n+1/2}}\Big((\rho\tilde{s}_1)_i^{n+1}-(\rho\tilde{s}_1)_i^{n+\frac{1}{2}}\Big)=0, \tag{28}$$

where

$$\begin{aligned}(\rho\tilde{s}_2)_i^{n+\frac{1}{2}} &= (\rho\tilde{s}_2)_i^n-\tfrac{\Delta t}{\Delta x}\left(\phi_{i+\frac{1}{2}}^{\rho\tilde{s}_2}-\phi_{i-\frac{1}{2}}^{\rho\tilde{s}_2}\right),\\ \beta_i &= \beta\Big((\tilde{T}_1)_i^{n+1/2},(\tilde{T}_2)_i^{n+1/2}\Big),\\ (\tilde{T}_k)_i^{n+1/2} &= \frac{(\rho_i^{n+1})^{\gamma_k-1}}{\gamma_k-1}\mathrm{e}^{-(\tilde{s}_k)_i^{n+1/2}}.\end{aligned}$$

The above nonlinear problem in the unknown $(\rho\tilde{s}_1)_i^{n+1}$ can be shown to admit a unique solution as soon as the approximate Riemann solver involved in the first step obeys discrete entropy inequality for the Lax pair $(\rho\tilde{s}_2,\rho\tilde{s}_2u)$. This in turn uniquely defines $(\rho\tilde{s}_2)_i^{n+1}$ according to:

$$(\rho\tilde{s}_2)_i^{n+1}=\{\rho\tilde{s}_2\}\Big(\mathbf{w}_i^{n+1},(\rho\tilde{s}_1)_i^{n+1}\Big).$$

When $\phi^{\mathbf{w}}$ is computed by an approximated Riemann solver, then, following the principle proposed in [27], the fluxes $\phi_{i+\frac{1}{2}}^{\rho\tilde{s}_1}$ and $\phi_{i+\frac{1}{2}}^{\rho\tilde{s}_2}$ are computed in order to ensure a maximum principle. In addition, we have (see [10] for the proof):

Theorem 3 *We assume that the scheme (25) is entropic and satisfies a maximum principle for the specific entropies. Under the CFL restriction (24), the following discrete entropy inequalities are satisfied:*

$$\{\rho\Psi_k(\tilde{s}_k)\}(\mathbf{w}_i^{n+1})-(\rho\Psi_k(\tilde{s}_k))_i^n +\frac{\Delta t}{\Delta x}\Big\{\{\rho\Psi_k(\tilde{s}_k)u\}_{i+1/2}^n-\{\rho\Psi_k(\tilde{s}_k)u\}_{i-1/2}^n\Big\}\le 0,$$

for any strictly increasing functions Ψ_k assumed to satisfy the convexity of the maps $\mathbf{w}\to\rho\Psi_1(\tilde{s}_1)$ and $\mathbf{w}\to\rho\Psi_2(\tilde{s}_2(\mathbf{w}))$. The following maximum principles for the specific entropies are met:

$$(\tilde{s}_k)_i^{n+1}\le\max((\tilde{s}_k)_{i-1}^n,(\tilde{s}_k)_i^n,(\tilde{s}_k)_{i+1}^n),\quad k=1,2. \tag{29}$$

The partial specific internal energies $(\tilde{\epsilon}_1)_i^{n+1}$ and $(\tilde{\epsilon}_2)_i^{n+1}$ stay positive as soon as the density ρ_i^{n+1} is positive and the maximum principles $0\le(Y_{1,2})_i^{n+1}\le 1$ are satisfied.

4.2 Multidimensional formulations

The multidimensional problems do not introduce additional difficulties except usual difficulties in multidimensional approximations of standard Navier-Stokes or Euler equations (see Quirk [32], Berthon and Nkonga [12] or Toro [37]). The extension of the proposed models in 2D and 3D is given by:

$$\begin{cases} \partial_t \rho + \nabla.(\rho \mathbf{u}) = 0, \\ \partial_t \rho \mathbf{u} + \nabla.(\rho \mathbf{u} \otimes \mathbf{u}) + \nabla(\tilde{p}_1 + \tilde{p}_2) = 0, \\ \partial_t E + \nabla.(E + \tilde{p}_1 + \tilde{p}_2)\mathbf{u} = 0, \\ \frac{\beta}{T_2}\left\{\partial_t \rho \tilde{s}_1 + \nabla.(\rho \tilde{s}_1 \mathbf{u})\right\} - \frac{1-\beta}{T_1}\left\{\partial_t \rho \tilde{s}_2 + \nabla.(\rho \tilde{s}_2 \mathbf{u})\right\} = 0, \end{cases} \tag{30}$$

where for the bifluid β is given by algebraic formula (15) and for the diphasic model by the equation: $\partial_t \rho\beta + \nabla.(\rho\beta\mathbf{u}) = 0$. We consider in the sequel only the case where β defined by (15). Indeed, other approximations can be derived from this case.

Following the 1-D case, the problem to be solved in the first step of the splitting is:

$$\begin{cases} \partial_t \rho + \nabla.(\rho \mathbf{u}) = 0, \\ \partial_t \rho \mathbf{u} + \nabla.(\rho \mathbf{u} \otimes \mathbf{u}) + \nabla(\tilde{p}_1 + \tilde{p}_2) = 0, \\ \partial_t E + \nabla.(E + \tilde{p}_1 + \tilde{p}_2)\mathbf{u} = 0, \\ \partial_t \rho \tilde{s}_1 + \nabla.(\rho \tilde{s}_1 \mathbf{u}) = 0. \end{cases} \tag{31}$$

The variable $\mathbf{W} = {}^t(\rho, \rho\mathbf{u}, E)$ is updated as follows:

$$\mathbf{W}_i^{n+1} = \mathbf{W}_i^n - \frac{\Delta t}{a_i} \sum_{j \in \vartheta(i)} \phi_{ij},$$

where a_i is the area, $\vartheta(i)$ the set of neighboring cells of cell i. The numerical flux ϕ_{ij} is computed from the exact or the approximated solution of the Riemann problem stated at the cell interface:

$$\phi_{ij} = \phi\Big(\mathbf{n}_{ij}, \mathbf{W}_i, (\rho\tilde{s}_1)_i, \mathbf{W}_j, (\rho\tilde{s}_1)_i\Big),$$

where $\mathbf{n}_{ij}$ is the normal to the cell interface between cells i and j. The second step of the splitting is now given by:

$$\frac{(\beta_1)_i}{(T_1)_i}\Big(\{\rho\tilde{s}_2\}(\mathbf{W}_i^{n+1},(\rho\tilde{s}_1)_i^{n+1})-(\rho\tilde{s}_2)_i^n+\frac{\Delta t}{a_i}\sum_{j\in\vartheta(i)}\phi_{ij}^{\rho\tilde{s}_2}\Big)-$$
$$\frac{(\beta_2)_i}{(T_2)_i}\left((\rho\tilde{s}_1)_i^{n+1}-(\rho\tilde{s}_1)_i^n+\frac{\Delta t}{a_i}\sum_{j\in\vartheta(i)}\phi_{ij}^{\rho\tilde{s}_1}\right)=0. \tag{32}$$

The extension of the nonlinear projection scheme to multi-dimension is thus achieved.

4.3 Source terms

Source terms can be added in the model in different ways. In the turbulent models there are source terms associated to the turbulent pressure production. In the presence of external forces (gravity, ...) source terms model the total momentum production in a specific direction.

In any case, we assume that the size of source terms is small compared to dynamic of the flow (governed by the hyperbolic system). Therefore, the numerical approximation is achieved by a splitting technic. The system solved in the additionnal step is :

$$\partial_t\mathbf{w}=\dot{\mathbf{w}},\quad \partial_t(\rho\tilde{\mathbf{s}})=\rho\dot{\mathbf{s}}.$$

For the case of external forces for example, the previous production term is reduced to (multidimensional case):

$$\dot{\mathbf{w}}=\rho\begin{pmatrix}0,\\ \mathbf{g},\\ \mathbf{g}\cdot\mathbf{u}\end{pmatrix}\quad\text{and}\quad\dot{\mathbf{s}}=0$$

This system is integrated analytically. If $\mathbf{w}_i^m$ is the initial value and $\mathbf{g}$ assume linear ($\mathbf{g}=\mathbf{a}_0+\mathbf{a}_1t$), we obtain:

$$\mathbf{w}_i^{m+1}=\mathbf{w}_i^m+\rho_i^m\begin{pmatrix}0\\ (t^{m+1}-t^m)\mathbf{a}_0\\ \frac{(t^{m+1}-t^m)^2}{2}\mathbf{a}_0\cdot\mathbf{u}_i^m\end{pmatrix}+\rho_i^m\begin{pmatrix}0\\ \frac{(t^{m+1}-t^m)^2}{2}\mathbf{a}_1\\ \frac{(t^{m+1}-t^m)^3}{6}\mathbf{a}_1\cdot\mathbf{u}_i^m\end{pmatrix}.$$

Generalization to the polynomial case $\mathbf{g}=\sum\mathbf{a}_kt^k$ is straightforward. So that, we can perform computations where the general external forces are substituted by its time expansion.

5 Numerical results

In this section we focus on the bifluid model for perfect gases at the vanishing viscosity limits where the fraction is given by (15). The parameters m_1 and m_2 are fixed equal to 5 while $\bar{\mu}$ is set equal to one. This model is numerically applied to three test cases: the 1D shock tube, the 2D shock-bubble interaction and the tank filling. The numerical fluxes are computed by the Roe approximated Riemann solver (see Roe [35]). For 2D computations, we use unstructured triangular meshes, and the control volumes are of *cell vertex* type (see Nkonga [31]). The computations are performed with a first order and second order approximations using a MUSCL type technique in the time evolution step of the splitting. In order to preserve entropy inequalities, the nonlinear projection step is always approximated by a first order scheme.

5.1 Shock tube

We consider the initial data for a bifluid Riemann problem given by $\mathbf{u}_L$ for $x < 0$ and $\mathbf{u}_R$ for $x > 0$ with:

$$\mathbf{u}_L = \begin{pmatrix} \rho_L = 1000 \\ u_L = 0 \\ (\tilde{p}_1)_L = 10^5 \\ (\tilde{p}_2)_L = 0 \end{pmatrix} \quad \text{and} \quad \mathbf{u}_R = \begin{pmatrix} \rho_R = 534.18 \\ u_R = -11.56 \\ (\tilde{p}_1)_R = 0 \\ (\tilde{p}_2)_R = 57974.44 \end{pmatrix}.$$

The adiabatic exponents are $\gamma_1 = 5/3$ and $\gamma_2 = 7/5$.

The associated **exact** solutions thus correspond to smooth regularizations of Riemann solutions for the underlying first order system extracted from (1). They are thus made up generally speaking of the juxtaposition of traveling wave solutions and "rarefaction" solutions. We do not develop the way to obtain the exact solutions. But we just indicate that the exact solutions are obtained when integrating, using Maple subroutines, the ODE's system for governing traveling wave solutions (see [9] or [11] to further details). After Raviart and Sainsaulieu [34], in the limit of a rescaling parameter, the exact solutions of the Riemann problem for the hyperbolic system (1) compatible with the diffusive tensor are thus obtained.

The exact solution is composed of a shock wave traveling in the left hand gas and a shock wave traveling in the right hand gas. The material interface is given by the contact discontinuity.

The domain is one meter long and is discretized with 500 cells. The calculation is performed with a CFL number equal to 0.5. In figures 1 and 5, the solution is displayed at time 0.02 second. There is a good agreement between the exact solution and the approximate solution obtained by the nonlinear projection scheme (figure 1). Second order results obtained by the usual MUSCL technique are comparable to the exact solution and the first order approximation (figures 3 and 4). Due to the nonlinear projection step that is always first order accurate, the differences between the first and the second order approximations are relatively small. At the contrary, numerical schemes where non conservative products are computed as source terms (not included in the Riemann Solver [30]), induce very large errors (figure 5). These behaviors of the classical schemes persist with mesh refinements and for high order methods. Indeed, in these methods all the non conservative products are dropped in the source term with some *ad hoc* finite difference approximations (for instance, see [30]).

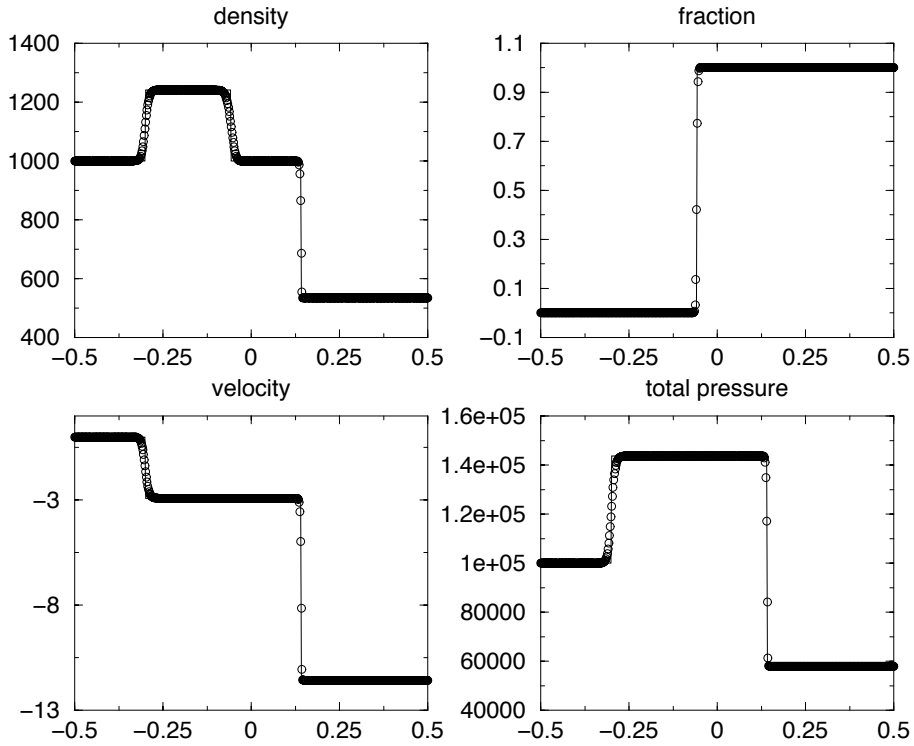

Fig. 1. Riemann problem: comparison between exact solution (fill line) and nonlinear projection scheme (circle symbol).

5.2 Bubble-shock interaction

Let us consider a "2D bubble" initially in equilibrium in the surrounding perfect gas with $\gamma = 1.4$. Initially, the bubble is located at $x = 0.05$ and $y = 0.05$; its radius is equal to 0.035. A shock coming from the left of the

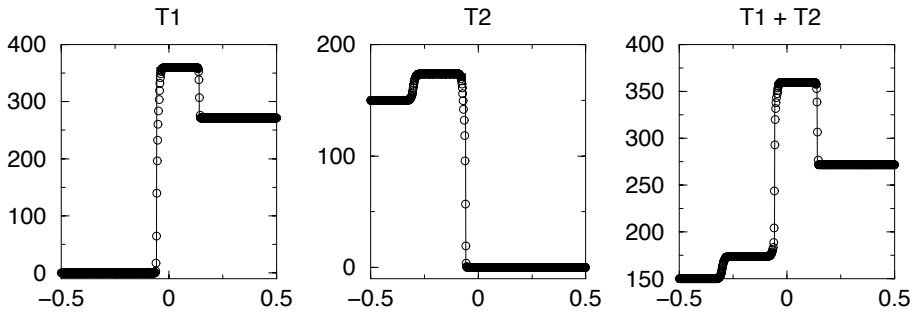

Fig. 2. Riemann problem: Profiles of the partial temperatures for the exact solution (fill line) and nonlinear projection approximation (circle symbol).

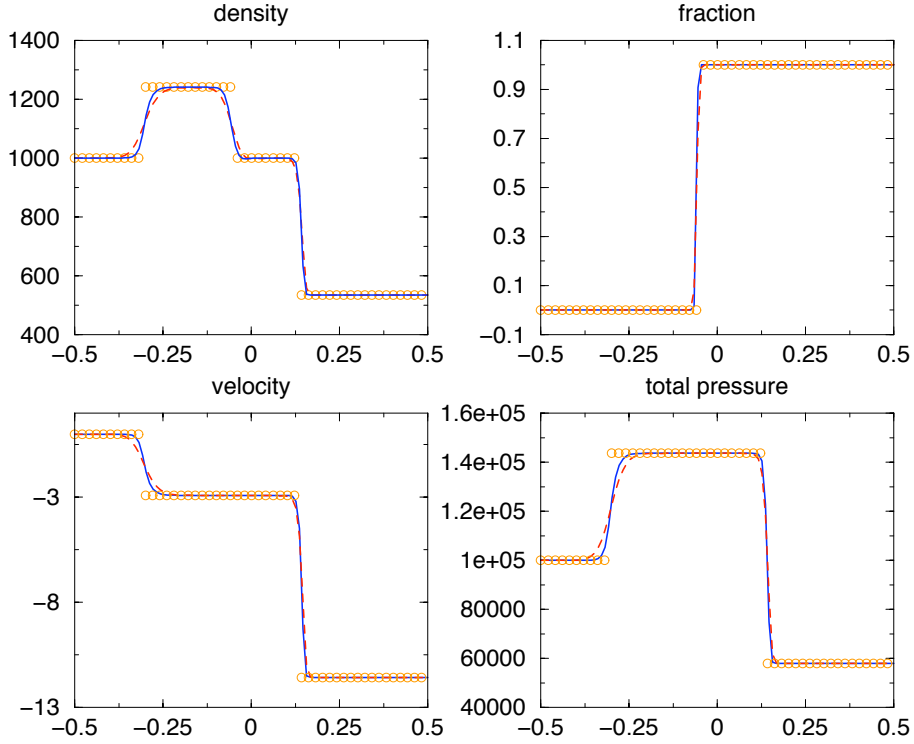

Fig. 3. Riemann problem, 100 cells mesh: Comparison between for the exact solution (circle symbol), the first order (dashed line) and the second order (fill line) nonlinear projection approximation

bubble is characterized by a Mach number $M_S = 1.22$:

$$\rho_{shock} = 3.4, \quad u_{shock} = 2.14, \quad v_{shock} = 0, \quad p_{shock} = 7.48.$$

The numerical data used here are similar to the one proposed by Quirk and Karni [33]. The computational domain is a rectangle of size $L_x = 0.3$ m and $L_y = 0.1$ m. The mesh is composed of 30,400 vertex and 600,000 triangles corresponding to a 300x100 structured mesh.

We propose two numerical simulations for which the corresponding experiments were first conducted by Haas and Sturtevant [22].

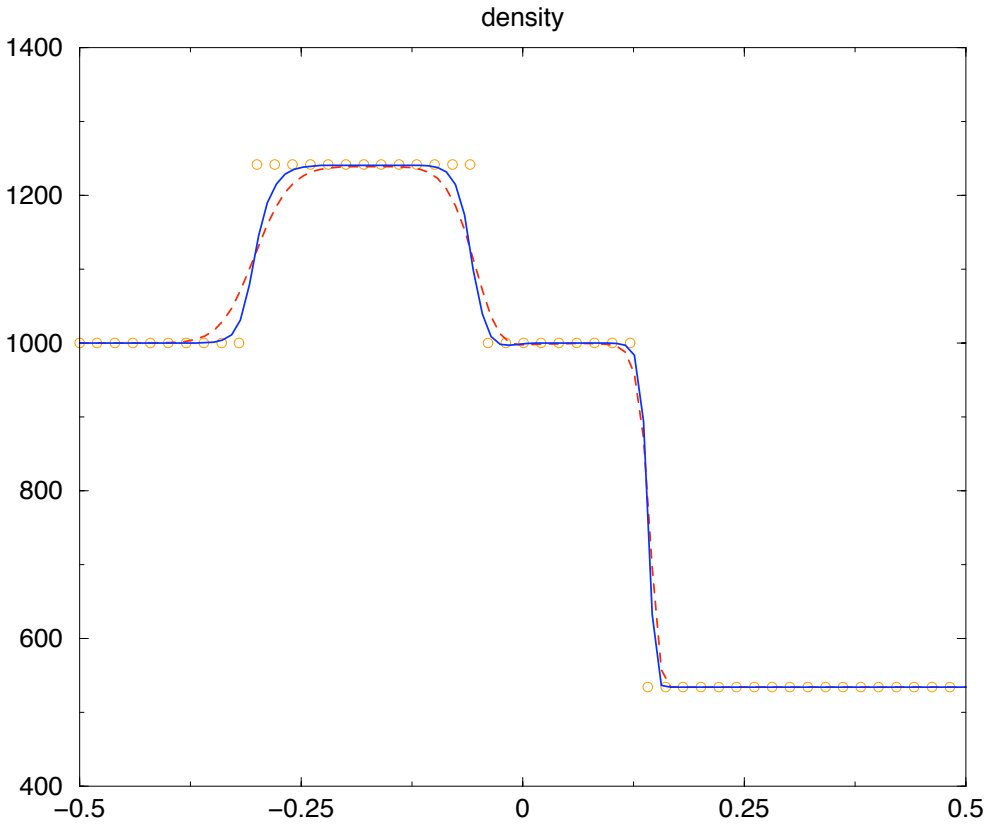

Fig. 4. Riemann problem, 100 cells mesh: Comparison between the exact solution (circle symbol), the first order (dashed line) and the second order (fill line) nonlinear projection approximation.

In the first simulation (figure 7), the bubble gas is helium ($\gamma = 1.6$) at the initial density $\rho_{He} = 0.138$. In the second simulation (figure 8), the bubble gas is Refrigerant 22 ($\gamma = 1.25$) at the initial density $\rho_{R22} = 3.154$. In both cases and without any additional numerical procedures, the material interface does not produce spurious waves.

In the first case, the bubble density is lower than the surrounding gas density ($\rho_{gaz} = 1$) while in the second case it is higher. In any case, numerical behavior is in accordance with the dynamics of the bubble-shock interaction observed in the physical experiment by Haas and Sturtevant [22]. Let us just recall that whereas the helium bubble is lighter than the surrounding gas and so acts as a divergent acoustic lens (strong deformation of the bubble into a vortex pair), the R22 bubble is heavier and therefore acts as a convergent acoustic lens.

5.3 Tank filling

The last numerical application is devoted to the tank filling. The tank is defined by two cylinders centered at the origin with the radius 0.2 and 0.15 (figure 9).

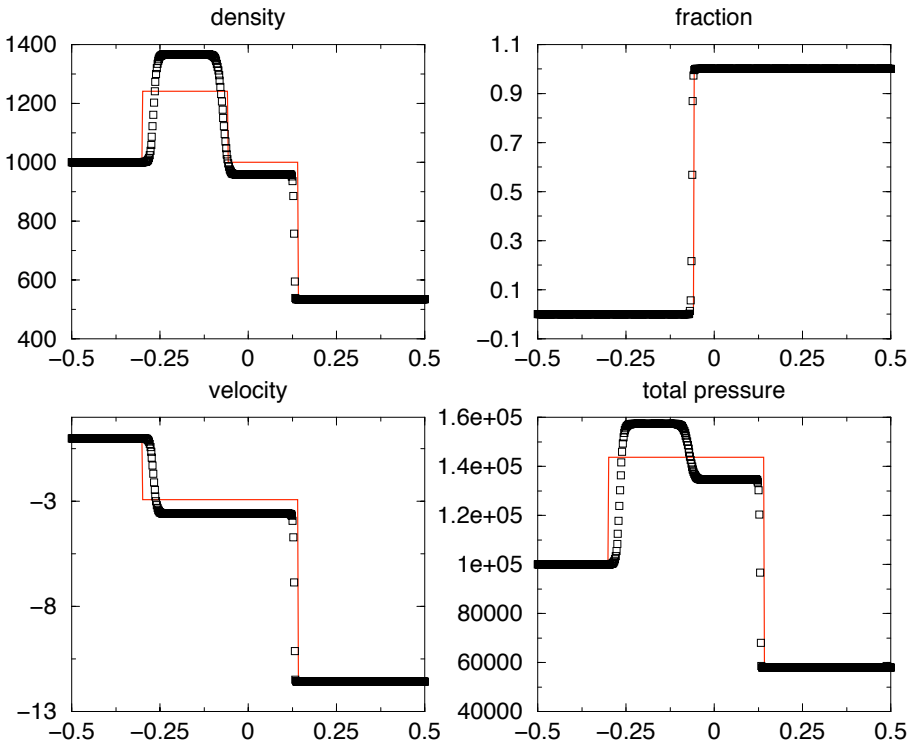

Fig. 5. Riemann problem: comparison between exact solution (fill line) and classical scheme (square symbol).

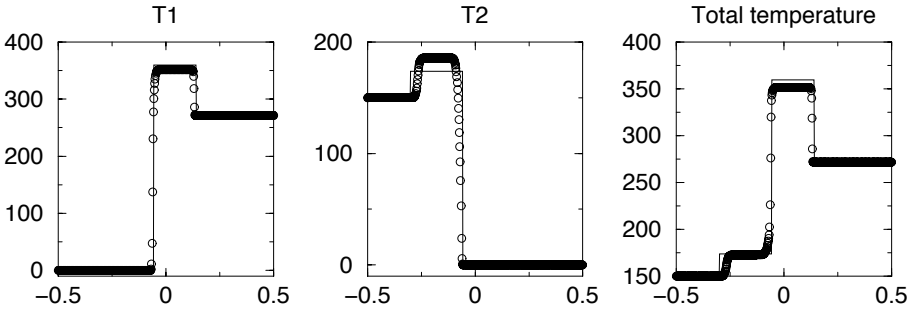

Fig. 6. Riemann problem: Profiles of the partial temperatures the exact solution (fill line) and classical scheme approximation (circle symbol).

Initially, the tank contains a perfect gas ($\gamma = 5/3$) at rest and at the atmospheric pressure with a density $\rho = 1$. There is a valve on the external cylinder centered at $x = -0.2$ and $y = 0$ with radius 0.006. Then, an other perfect gas ($\gamma = 7/5$) with density $\rho = 1000$ injected in the tank at a constant velocity 1 $m.s^{-1}$ in the (Ox)-direction.

The main difference with the other test cases is that the material interface is created by the boundary condition and the gravity is active in the (Oy)-direction. The obtained solution is conform to the expected physical behavior.

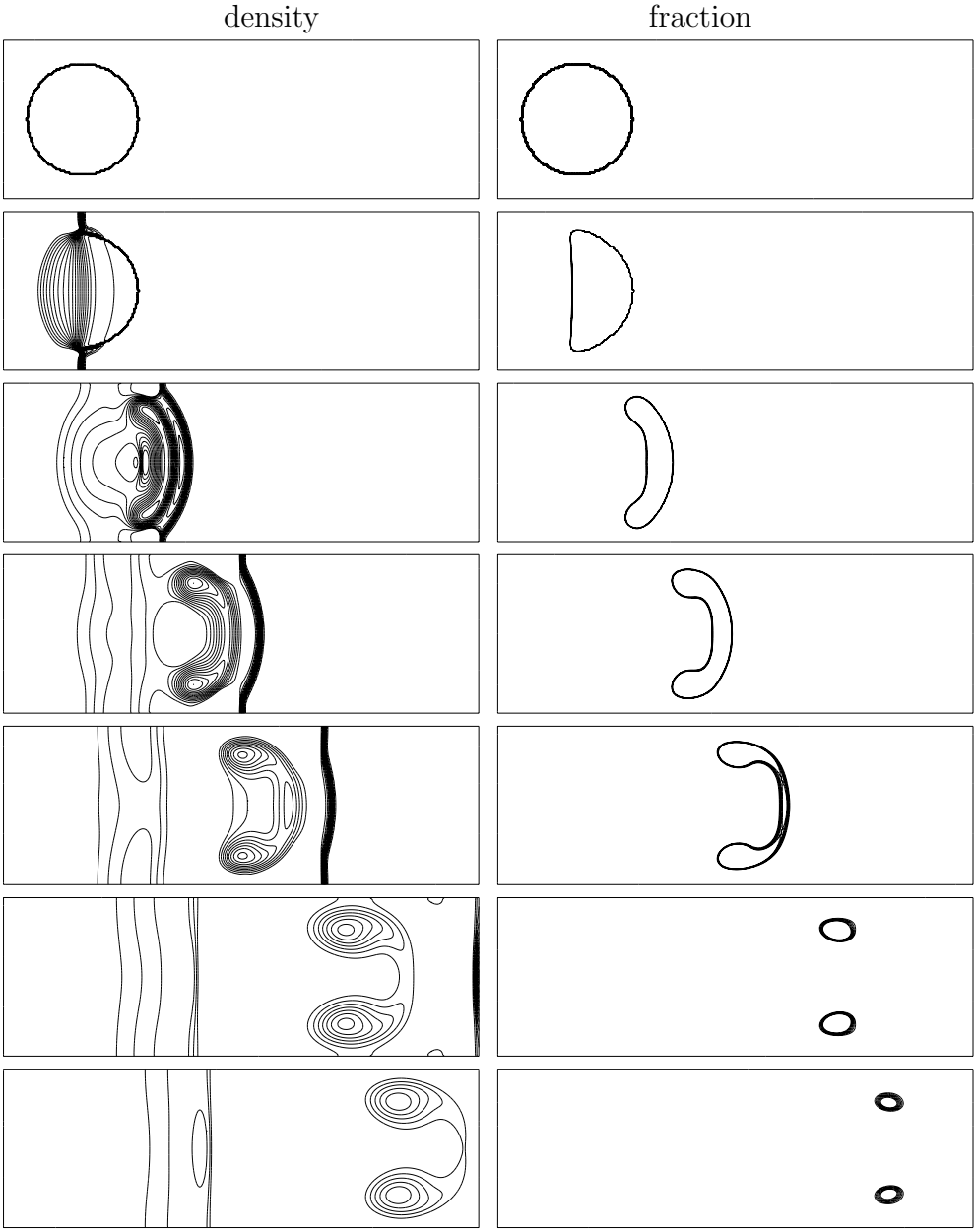

Fig. 7. Density and material interface for interaction of an $M_S = 1.22$ shock wave with an He cylindrical bubble. Respective times: $16\mu s$, $31\mu s$, $47\mu s$, $64\mu s$, $94\mu s$ and $110\mu s$.

6 Conclusion

We have proposed a numerical strategy for the numerical modeling of non-mixing multifluid flows. The physical model is a reformulation of the model proposed by Karni [24,25] based on both the multi-pressure (see Berthon and Coquel [10]) and the reduced multiphase models, proposed respectively by Berthon and Coquel [10] and Massoni et al. [29]. The final model conserves

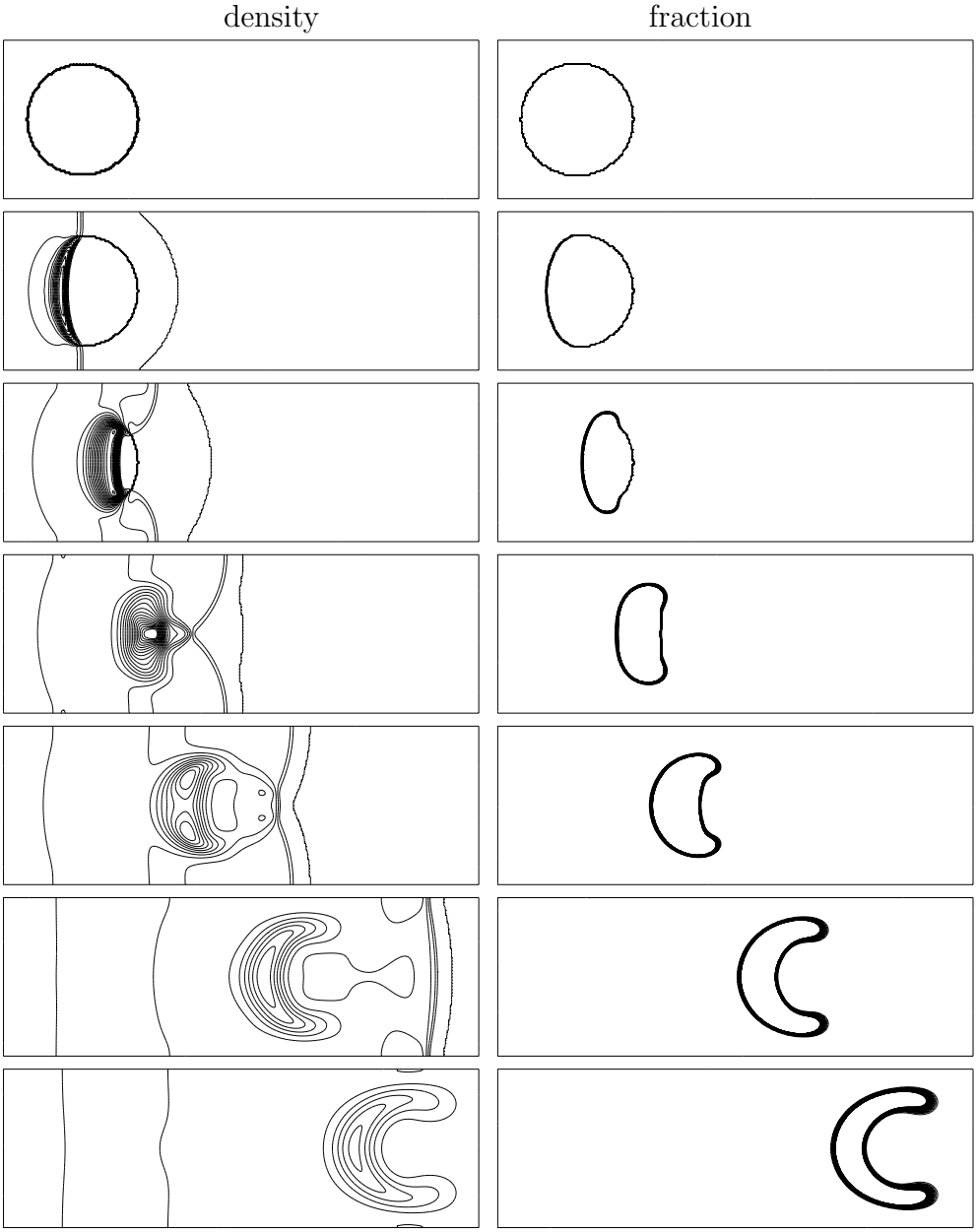

Fig. 8. Density and material interface for interaction of an $M_S = 1.22$ shock wave with an R22 cylindrical bubble. Respective times: $16\mu s$, $31\mu s$, $47\mu s$, $63\mu s$, $94\mu s$ and $126\mu s$.

the mass, momentum and energy of the mixture, completed by non conservatives balance equations coupling the entropy dissipation rate of the flow components. This model, in general, cannot be formulated in a fully conservative form. The numerical method based on the nonlinear projection step, enforces the validity of the entropy balance equations at the discrete level. Furthermore, the approximated solutions satisfy the required positiveness preserving properties in addition to several stability requirements. The shape of the viscous tensor is an important parameter of the numerical model. In the

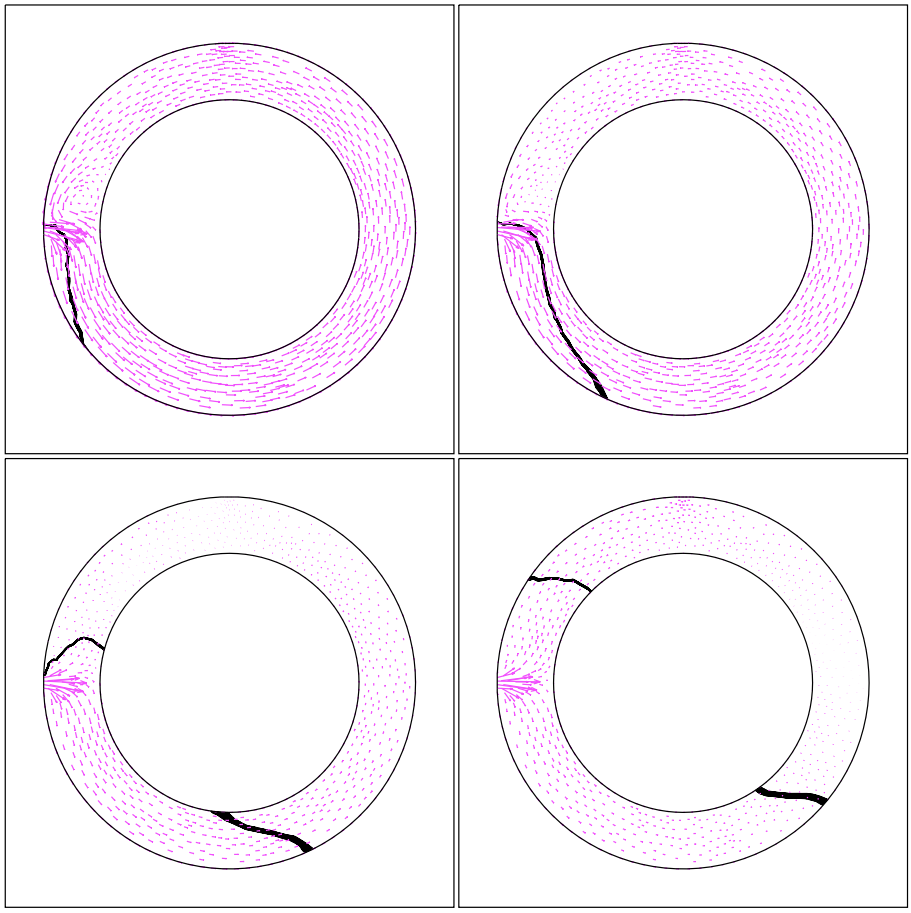

Fig. 9. Tank filling: velocity field and material interface.

vanishing viscosity limit, the numerical solutions are consistent with physics when the classical methods converge to non physical solutions. The efficiency of the numerical model is demonstrated by 1D and 2D applications on unstructured meshes. The future work will be the improvement of the method for turbulent miscible multifluid flows.

References

[1] R. Abgrall, How to prevent pressure oscillations in multicomponent flow calculations: a quasi-conservative approach *J. of Comp. Phy.*, **125** (1996), no. 1, pp. 150–160.

[2] R. Abgrall, B. Nkonga, R. Saurel, Efficient numerical approximation of compressible multi-material flow for unstructured meshes, *Computers & Fluids*, **32** (2003), pp. 571–605.

[3] R. Abgrall, S. Karni, Computations of compressible multifluids, *J. of Comp. Phy.*, **169** (2001), pp. 594–623.

[4] R. Abgrall, R. Saurel, A simple method for compressible multifluid flows, *SIAM J. Sci. Comput.*, **21** (1999) No 3 1115–1145.

[5] R. Abgrall, R. Saurel, Discrete equations for physical and numerical compressible multiphase mixtures, *preprint LRC 01-13* (2001).

[6] R. Abgrall, R. Saurel, A multiphase Godunov method for compressible multifluid and multiphase flows, *J. of Comp. Phy.*, **150** (1999) 425–467.

[7] G. Allaire, S. Clerc, S. Kokh, A Five-Equation Model for the Simulation of Interfaces between Compressible Fluids, *J. of Comp. Phy.*, **181**, Issue 2 (2002), pp 577-616.

[8] N. Andrianov, R. Saurel, G. Warnecke, A simple method for compressible multiphase mixtures and interfaces, *Rapport de recherche de l'INRIA*, RR-4247 (2001).

[9] C. Berthon, F. Coquel, About shock layers for compressible turbulent flow models, *preprint MAB 01-29* (2001).

[10] C. Berthon, F. Coquel, Nonlinear projection methods for multi-entropies Navier-Stokes systems, *Innovative methods for numerical solutions of partial differential equations* (Arcachon, 1998), pp. 278–304, World Sci. Publishing, River Edge (2002).

[11] C. Berthon, F. Coquel, Travelling wave solutions of a convective diffusive system with first and second order terms in nonconservation form, *Hyperbolic problems: theory, numerics, applications*, Vol. I (Zürich, 1998), pp. 47–54, Internat. Ser. Numer. Math., 129, Birkhäuser, Basel (1999).

[12] C. Berthon, B. Nkonga, Incompatible numerical viscous limit for systems of conservation laws, *preprint LRC 02-18*, Finites Volumes for Complex Applications III pp. 139–146 (2002).

[13] C. Berthon, B. Nkonga, *work in preparation.*

[14] C. Berthon, D. Reignier, A combustion Model and approximate nonlinear projection scheme, accepted in *M2AN* (2003).

[15] C. Chalons, Bilans d'entropie discrets dans l'approximation numrique des chocs non classiques. Application aux quations de Navier-Stokes multi-pression 2D et quelques systmes visco-capillaires, *PHD thesis*, Ecole polythecnique (Paris, France), 2002.

[16] F. Coquel and B. Perthame, Relaxation of energy and approximate Riemann solvers for general pressure laws in fluid dynamics, *SIAM, J. of Numer. Anal.*, 35, No 6, pp. 2223–2249, 1998.

[17] F. Coquel and C. Marmignon, Numerical methods for weakly ionized gas. *Astrophys. Space Sci.*, 260, No.1-2, 15-27. 1998

[18] G. Dal Maso, P. LeFloch and F. Murat, Definition and weak stability of a non conservative product, *J. Math. Pures Appl.*, 74, pp. 483–548, 1995.

[19] D. Drew and S. Passman, **Theory of multicomponent fluids**, Applied Mathematical Sciences, Vol 135, Springer 1998.

[20] E. Godlewski and P.A. Raviart, **Hyperbolic systems of conservations laws**, Applied Mathematical Sciences, Vol 118, Springer 1996.

[21] A. Harten, P.D. Lax and B. Van Leer, On upstream differencing and Godunov type schemes for hyperbolic conservation laws, *SIAM Review*, Vol 25, No 1, pp. 35–61, 1983.

[22] J. F. Haas and B. Sturtevant, Interaction of a weak shock wave with cylindrical and spherical gas inhomogeneities, *J. Fluid Mech.*, Vol 181, pp. 41–76, 1987.

[23] T. Y. Hou and P. G. LeFloch, Why nonconservative schemes converge to wrong solutions: error analysis, *Math. of Comp.*, Vol 62, No 206, pp. 497–530, 1994.

[24] S. Karni, A multicomponent flow calculations by a consistent primitive algorithm, *J. of Comp. Phys.*, **112** (1994) 31–43.

[25] S. Karni, Hybrid multifluid algorithms. , *SIAM J. Sci. Comput.*, **17**, No.5, 1019-1039 (1996)

[26] F. Lagoutière, Modélisation mathématique et résolution numérique de problèmes de fluides compressibles à plusieurs constituants, PhD Thesis, Université Paris VI (200).

[27] B. Larrouturou, How to preserve the mass fractions positivity when computing compressible multi-component flows, *J. Comput. Phys.* 95, No 1, pp. 59–84, 1991.

[28] B. Larrouturou and C. Olivier, On the numerical appproximation of the K-eps turbulence model for two dimensional compressible flows, *INRIA report*, No 1526, 1991.

[29] J. Massoni, R. Saurel, B. Nkonga and R. Abgrall, Proposition de methodes et modeles euleriens pour les problemes a interfaces entre fluides compressibles en presence de transfert de chaleur, *Journal of Heat and Mass Transfer*, **45** No 6, pp. 1287-1307 (2001).

[30] B. Mohammadi and O. Pironneau, **Analysis of the K-Epsilon Turbulence Model**, Research in Applied Mathematics, Masson Eds 1994.

[31] B. Nkonga, On the conservative and accurate CFD approximations for moving meshes and moving boundaries. *Comput. Methods Appl. Mech. Eng.*, 190, No.13-14, pp. 1801-1825 (2000).

[32] J. Quirk, A contribution to the great Riemann solver debate, *Int. J. Numer. Methods Fluids* vol. 18, No 6, 1994, pp. 555-574.

[33] J. Quirk and S. Karni, On the dynamics of a shock-bubble interaction, *J. Fluid Mech.*, Vol 318, pp. 129–163, 1996.

[34] P. A. Raviart and L. Sainsaulieu, A nonconservative hyperbolic system modeling spray dynamics. Part 1. Solution of the Riemann problem, *Math. Models Methods in App. Sci.*, 5, No 3, pp. 297–333, 1995.

[35] P.L. Roe, Approximate Riemann solvers, parameter vectors, and difference schemes. *J. Comput. Phys.* vol. 43, 1981, pp. 357-372.

[36] K. M. Shyue, An efficient shock-capturing algorithm for compressible multicomponent methods, *J. of Comp. Phys.*, **142** (1998) 208–242.

[37] E. F. Toro, Anomalies of conservative methods: analysis, numerical evidence and possible cures, *C. F. D. Journal* vol. 11, No 2, 2002, pp. 128-143.